Main S&T results/foregrounds

WP1: TPS design

The envisaged concept of the SMARTEES project was based on the integration of conventional and non-conventional parts to create a TPS technology sample with multifunctional properties such as oxidation protection, thermal protection, thermo-structural functionality, adjustable surface emissivity, insulation capability and in-plane controlled thermal conductance. This was planned to be carried out by the integration of materials at three levels, as depicted in Figure 1.1, left. The preliminary design was based on the integration of three main parts: ceramic multilayer system (SiC or ZrB_2/SiC multilayers), thermo-structural part (CMC/foam/CMC sandwich structure) and metallic frame (titanium alloy). The way of joining of these three parts is brazing technology (1st and 2nd level bonding). Considering the three described material layers and procedure for a multifunctional SMARTEES TPS sample a first preliminary design concept was suggested, illustrated in Figure 1.2.

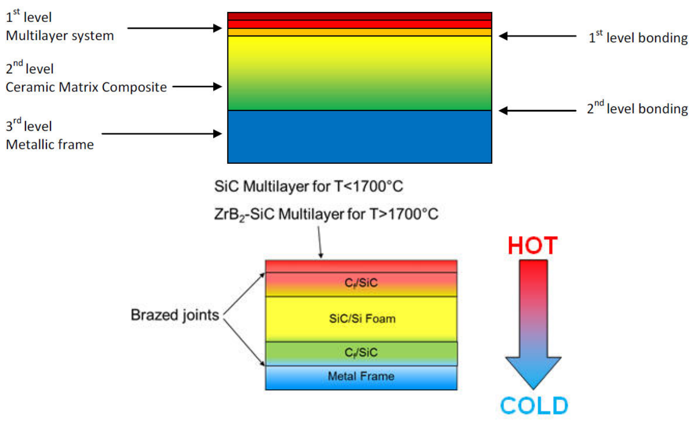

Fig. 1.1. Schematic TPS concept in an early stage (left) and preliminary design (right)

For the SMARTEES development work specification and requirements were selected and defined from ARV (advanced Reusable Vehicle) project which foresees implementation of a cargo transportation capability with the objective of being used for ISS cargo upload and download in support of ISS operations beyond 2016 (Figure 1.2, left). The concept retained for ARV shall not prevent nor impair its subsequent evolution towards a genuine crew transportation capability. A crew transportation version could become available in the 2025 timeframe. Within ARV project an APOLLO-type shape was selected and the heat shield was subdivided in two parts (see Figure 1.2, right): front shield with thermally high loaded areas and back shield which is moderately loaded.

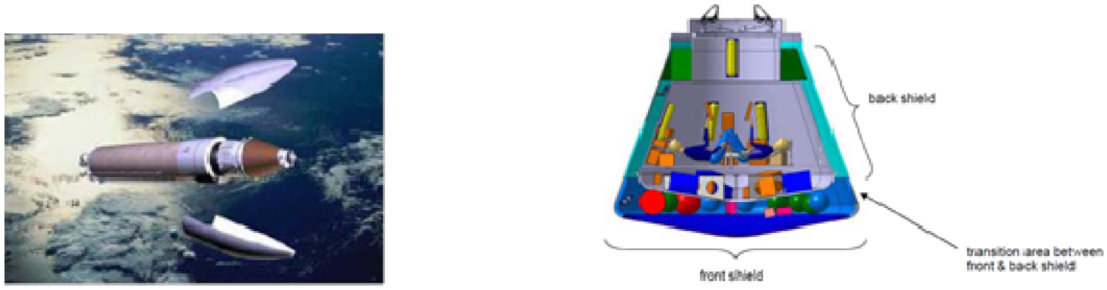

Fig. 1.2 ARV Cargo version (left) and ARV capsule with heat shield locations (right)

Two material options were available for the exposed multilayer level to be designed and developed with respect to different load case scenarios from ARV mission profile: SiC multilayers (suitable for temperatures T<1700 ºC) and ZrB_2/SiC multilayers (suitable for temperatures T>1700 ºC). Because of the nature of these two material options for the exposed outer surface layer two control points from ARV load case (LC) scenarios were selected for the design of the samples. Load Case 1 (LC1) is for a control point at the back shield where the corresponding heat fluxes and thermal loads (sizing trajectory) are moderate and therefore offer an interest for the SiC based materials. The temperature is approx. 1300 ºC and heat flux around 0.3 MW/m^2. Load Case 2 (LC2) is at the front shield with high heat fluxes and thermal loads (sizing trajectory) and therefore interesting for ZrB_2/SiC materials. The corresponding temperatures are approx. 1700-1800 ºC and heat fluxes around 0.8 MW/m^2. Considering the selected load case scenarios and defined TPS relevant requirements (thickness, aerial mass, emissivity, temperatures, thermal insulation capability, maximum temperature on vehicle structure, mechanical & thermo-mechanical stability under load conditions etc.), two solutions for LC1 and LC2 were designed. TPS technology sample size was defined first to $50x50mm^2$ for development and second $150x150mm^2$ for upscale. For LC1 a SiC multilayer without ZrB_2 and for LC2 a SiC/ZrB_2 multilayer with ZrB_2 layers intercalated among SiC layers (POLITO) was selected for the exposed top layer. For the integrated $CMC_{upper\ skin}$-SiSiC foam-$CMC_{lower\ skin}$ sandwich structure a continuous carbon fiber reinforced C_f/SiC material (SiCARBON™ from EADS) with a 2D-0°/90° architecture and a customized SiSiC foam (ERBICOL/SUPSI) with a defined pore size and orientation was used for both LC1 and LC2. The metallic stand-off was based on Ti_6Al_4V alloy (TECNALIA). The joints for SiC multilayer/$CMC_{upper\ skin}$ and $CMC_{lower\ skin}$/metallic stand-off were realized by brazing technology (TECNALIA/NCSRD). For thermal insulation a fibrous ceramic phase was selected to be filled into in the SiSiC foam (ERBICOL/SUPSI). Figure 1.3 shows the 3D models of the fully assembled technology samples for LC1 (left) and LC2 (right), illustrating the top SiC multilayer, the upper CMC skin, the SiSiC foam, the lower CMC skin and the metallic stand-offs (from the top to the bottom).

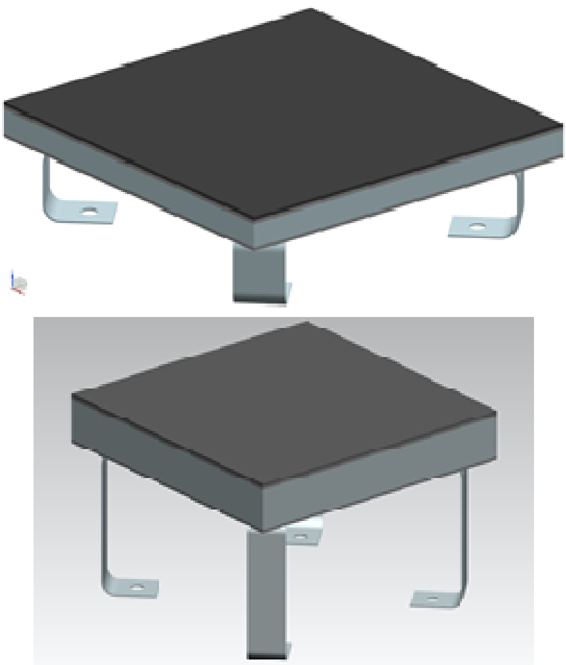

Figure 1.1: 3D model for LC1 design (left) and LC2 design (right), top view

WP2: Materials development and manufacturing

Three kinds of materials and the relevant manufacturing processes/technologies were developed during the project:

1. Ceramic laminates based on SiC (or SiC plus ZrB_2) mainly designed for oxidation protection
2. SiC-based foams (filled in by silica fibres) designed for thermal insulation
3. CMCs suitable to act as skin of SiC foams in a sandwich structure and designed for providing toughness and strength

1. Ceramic laminates based on SiC (or SiC plus ZrB_2) mainly designed for oxidation protection

A manufacture technology for multilayer ceramics was developed with the aim of granting to the part of TPS facing the atmosphere the following properties: oxidation and thermal shock resistance; high emissivity; thermal management capability; suitable strength, stiffness and hardness.

The processing path (Fig. 2.1) consisted of the following steps: green tape production by tape casting a suitable ceramic slurry containing proper sintering aids (E. Padovano, C. Badini, et al. "Pressureless sintering of ZrB_2-SiC composite laminates, using boron and carbon as sintering aids", Advances in Applied Ceramics,112, n°8 (2013) 478-486); formation of the green multilayer by stacking green tapes; de-binding thermal treatment; final sintering without the help of pressure.
The processing method based on tape casting allowed to developed several kinds of laminates (either with similar or dissimilar layers):

a) SiC multilayer
b) SiC-ZrB_2 composite multilayers showing different SiC:ZrB_2 ratios ranging from 100%SiC to 100% ZrB_2.
c) SiC laminates integrating porous layers for improving thermal insulation.
d) Hybrid laminates with C_f/SiC composite layers put in between SiC layers showing not-isotropic thermal conductivity (higher in the plane and lower through the thickness).
e) Hybrid laminates with alternate layers made of SiC and ZrB_2-SiC composite designed for alternating materials that are expected to display the best oxidation resistance in different temperature ranges (SiC up to 1600°C and ZrB_2-SiC composites over 1700°C).

Some mechanical features of different kinds of ceramic laminates are compared in table 2.1.

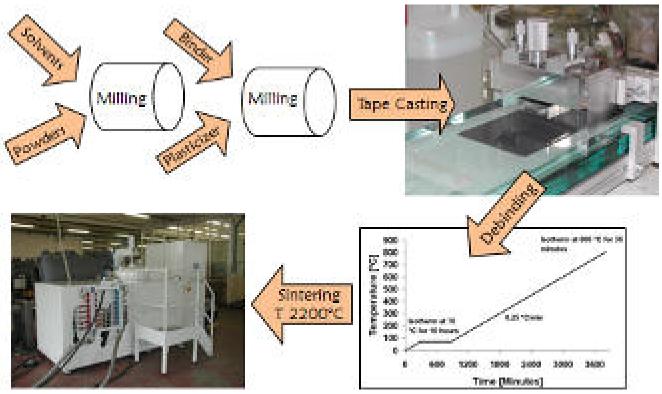

Fig. 2.1. Ceramic laminates processing path

Samples composition [% Vol.]	Elastic modulus [Gpa]	Bending strength [MPa]
100% SiC	339	324
40%SiC-60%ZrB_2	408	284
20%SiC-80%ZrB_2	444	277
100% SiC with 2 porous layers out of 10	240-270*	200-260*
SiC-C_f/SiC multilayer (2 composite layers out of 10)	288	288
20%SiC-80%ZrB_2 / SiC multilayer (2 composite layers out of 10)	310	263

*Depending on porosity degree in the porous layers

Tab. 2.1 Strength and stiffness of ceramic laminates.

The main results achieved for each multilayer concept developed in the frame of SMARTEES project are summarized in the following.

a) SiC multilayer: very good oxidation resistance in the temperature range 25-1600°C owing to the formation of a very thin and effective silica passive layer on the surface, quite good emissivity (C. Badini, et al "Oxidation behavior of laminate ceramics belonging to SiC-ZrB_2 system" in proc. 7th Workshop on Thermal Protection Systems and Hot Structures, Noordwjik, 8-10 April 2013 ESA ESTEC).

b) SiC-ZrB_2 composite multilayers: formation of a passive layer in every case but oxidation resistance in the temperature range 25-1600°C worsening with the ZrB_2 content increase; very high emissivity due to ZrB_2, even better than that displayed by SiC multilayer; expected better oxidation resistance over 1700°C due to the formation of ZrO_2 which does not melts up to 2700°C, contrary to silica which melts and then evaporates over 1700°C.

c) SiC laminates integrating porous layers: the presence of porous layers can halves the thermal conductivity through the thickness.

a) SiC laminates with C_f/SiC composite layers: composite layers provide enhanced conductivity in the plane and decrease of conductivity through the thickness (Fig. 2.2; W.S. Yang, C. Badini et al. “Thermophysical properties of short carbon fiber/SiC multilayer composites prepared by tape casting and pressureless sintering”, Int. J. Appl. Ceram. Technol., (2013) DOI: 10.111/ijac.12149).

d) Laminates with alternate layers made of SiC and ZrB_2-SiC: the ZrB_2-SiC composite layers are integrated in the multilayer structure with the aim of delaying the oxidation when temperature exceeds 1700°C and therefore the recession of SiC layers occurs; nevertheless the oxidation resistance up to 1600°C is well assured by the SiC skin (Fig. 2.3).

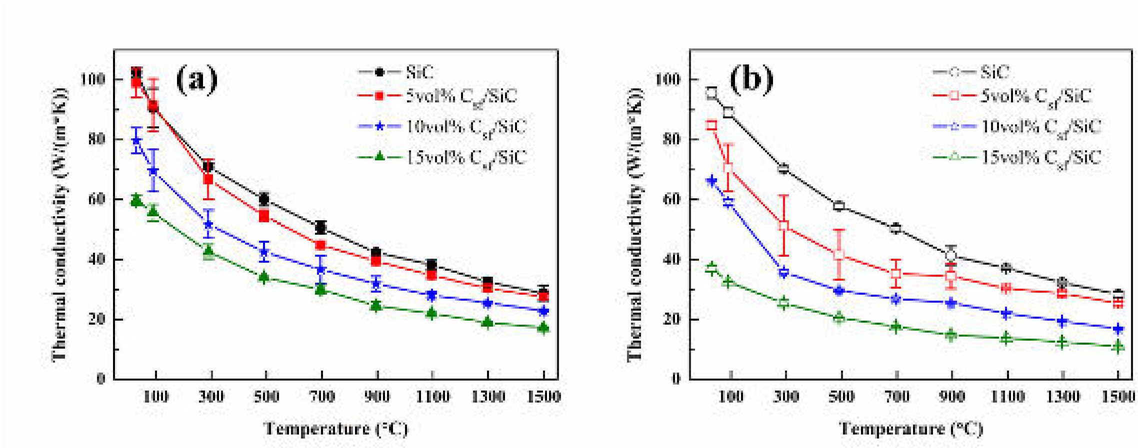

Fig.2.2 Thermal conductivities of SiC multilayer and Csf/SiC multilayer composites in Z direction from 30 to 1500 °C (a) before and (b) after oxidation treatment at 1500°C.

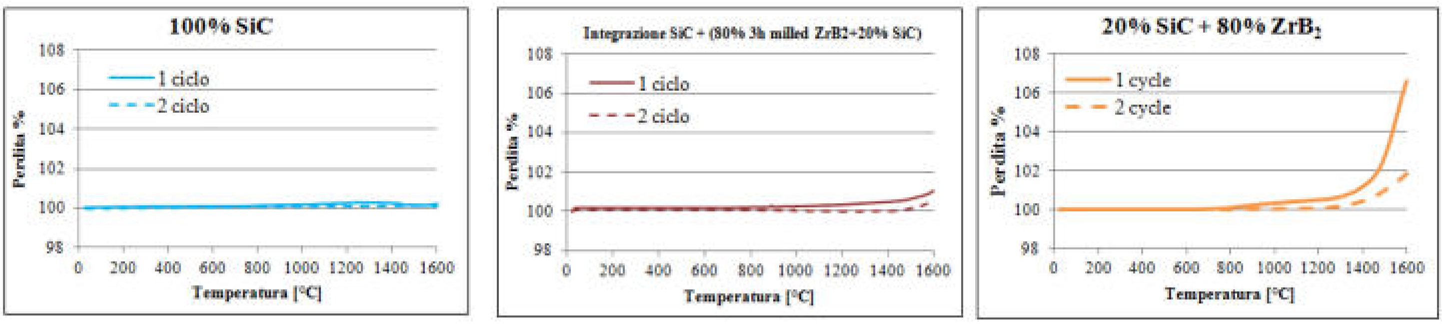

Fig.2.3. TGA curves under flowing air up to 1600°C: passive layer formation after the first heating run.

The manufacture process of these ceramic laminates has been based on tape casting technology because this technology has been adopted at industrial plant level since many years and it is well suitable for processing hybrid laminates with layers showing different microstructure and composition. Anyway in the frame of SMARTEES project the processing method parameters were adjusted in order to perform the up-scaling required for the production of the TPS at the technological sample level (WP5, Fig. 2.4).

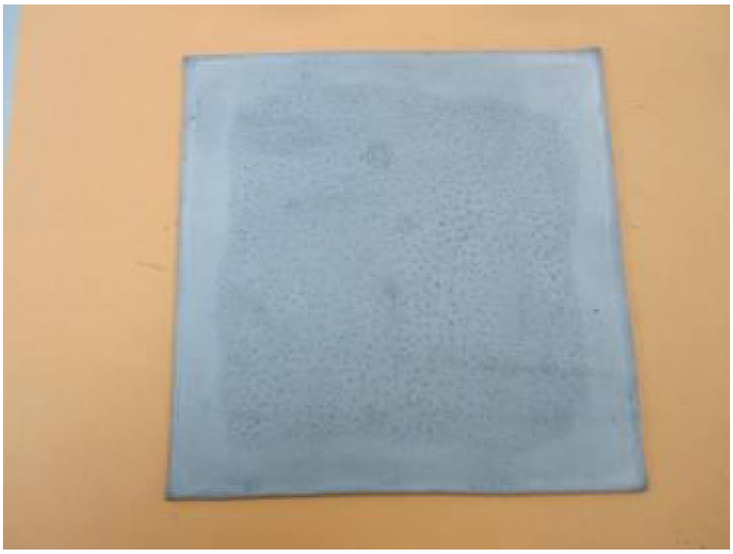

Fig. 2.4. Tiles 150X150X1.8 mm3, ten SiC layers.

In addition to the pressure-less sintering, other alternative process for the sintering of multilayers is the **Spark Plasma Sintering**. Spark plasma sintering (SPS) is found to compact powders satisfactorily through the simultaneous application of direct current pulses of high intensity and pressure. The electric current induces a temperature elevation within the sample by Joule's effect. The whole process lasts just a few minutes.

The consolidation experiments were performed at TECNALIA in a FCT Spark Plasma Sintering furnace (model S8451). This equipment can supply a direct current of 10000 A of intensity under a maximum tension of 10 V. The DC current was applied with pulse time of 10 ms and a pause time of 5 ms. The powder was filled in a graphite die between two graphite punches. The diameter of the samples was 20 or 30 mm. During the tests, the chamber was maintained under vacuum (10^{-2} Pa). Temperature was controlled by a pyrometer that measures the temperature in the interior part of the graphite punch. The maximum temperature was between 1700-1900 ºC during 1 min of holding time. The load (50 MPa) was applied during the heating.

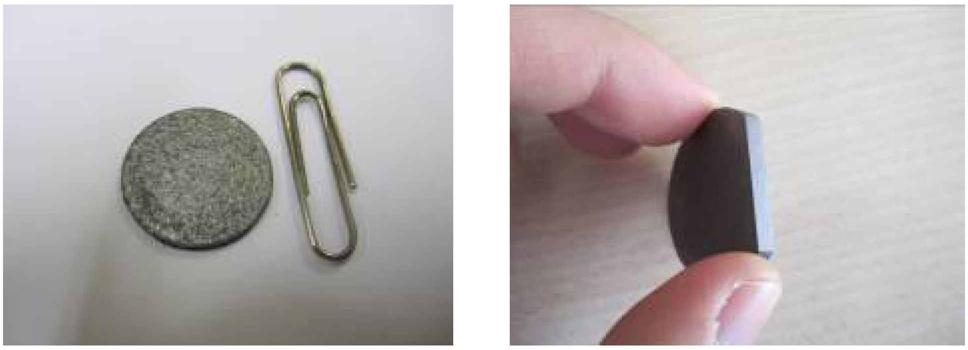

A B

Fig. 2.5. SPS samples A) Diameter 20 mm, B) Diameter 30 mm.

Main conclusions of the SPS tests are:

e) With monolithic materials (pure SiC, pure ZrB2 and SiC with carbon fibres), the temperature to obtain the maximum density depends on the composition. For SiC and SiC + Cf, this maximum densification (around 92 % of the theoretical density) was obtained at around 1850 ºC, however, for pure ZrB2 was necessary to reach 1900 ºC. As sintering aids B4C, TiC, C and B were used and it was not observed significant different between them. In all cases the porosity was very small and well distributed. In the case of the SiC with carbon fibres, the interface between the fibre and the SiC was very good, due to the fact that it is not possible to observe cracks or porosity between both materials.

f) Different configurations of multilayers were successfully obtained (see figure 2.6). The most important problem was the presence of cracks after the sintering. The reason of this cracks are the stresses produced by the difference in CTE during the fast cooling. The most successful way to avoid the cracks was the change of the load cycle. It was necessary to release the pressure at high temperature, to release the stresses produced by the difference in CTE.

g) The density of the composites was higher than the 90 % of the theoretical value. Small cracks were observed in the ZrB2/SiC layers. These cracks were perpendicular to the application of the load and it is believed that they are produced by the contraction of the layers during the fast cooling.

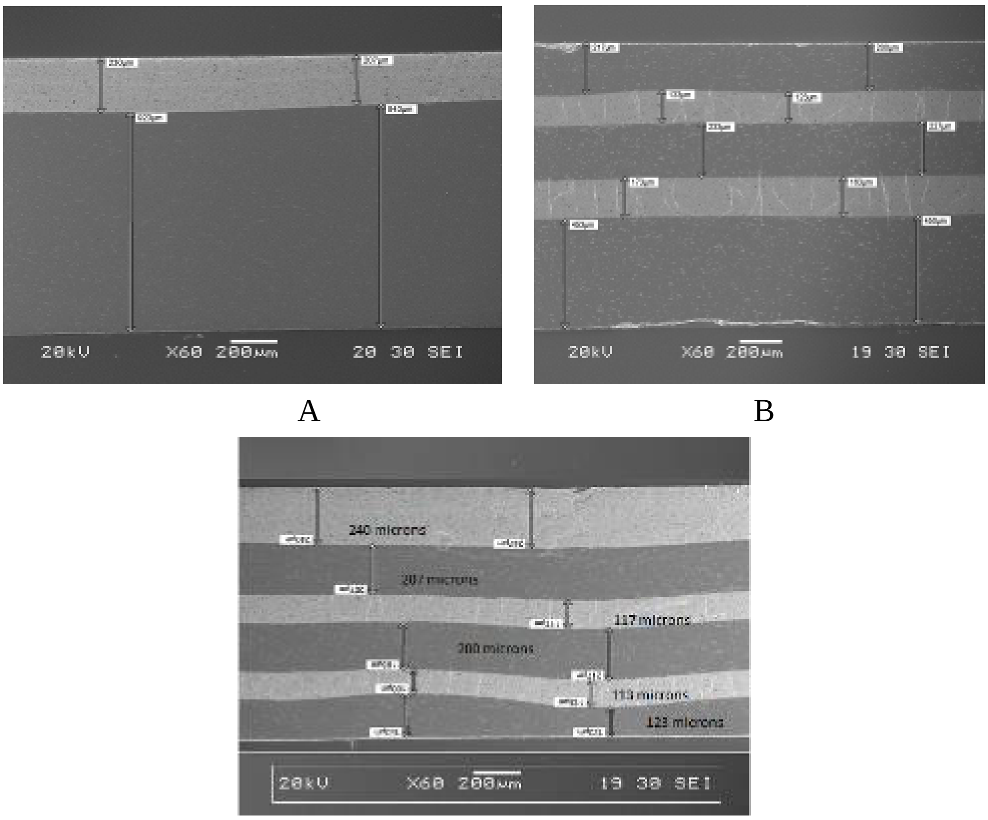

A B

C

Fig. 2.6. Different configurations of multilayers consolidated by SPS

2. SiC-based foams (filled in by silica fibres) designed for thermal insulation

For TPS applications, some carbides (e.g. SiC) are, for their outstanding thermo mechanical properties, the most appropriate. Reticulated SiC foams have an open pore structure with an interconnected network of cells, whose edges are made of solid struts. These foams can withstand long oxidative exposing conditions with low material degradation. The production method allows obtaining a microstructure composed of crystalline SiC and residual silicon with an open porosity smaller than 1%.

The material demonstrates high temperature stability up to 1400°C (air), resistance to acid and basic conditions, high thermal conductivity and thermal shock resistance.

The Erbicol standard foams are composed of 70% of SiC and 30% of free Si with pore size of 10 PPI. Erbicol, for the SiSiC foams production, uses a method called Schwarzwalder (Figure 2.7), which consists of the impregnation of a sacrificial polymeric template. The green body is then pyrolyzed in inert atmosphere and liquid silicon infiltrated under vacuum, which transforms the residual carbon in SiC.

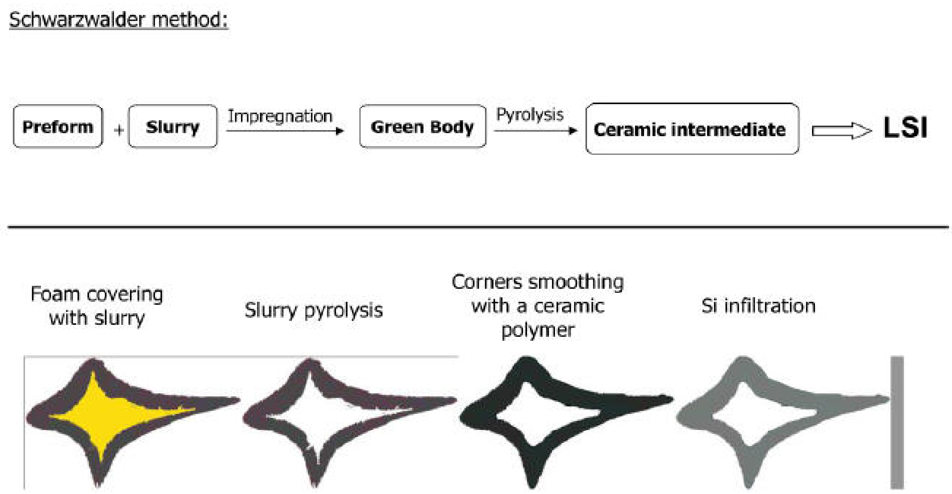

Figure 2.7. Section of a foam strut after impregnation, pyrolysis, densification and LSI.

In the table 2.2, material properties of standard 10 PPI foams are reported.

During the project, Erbicol produced different type of foams, optimizing material properties both at a microscopic and macroscopic level, aiming at producing the most performing and reliable product TPS application.

Property		Value
Foam Density	[gcm^{-3}]	0.323
Normalized Density		0.114
Macroporosity	[%]	88.6
Surface Area	[m^2 m^{-3}]	~ 500
Av. Strut Thickness	[mm]	0.9
Flexural Strength	[MPa]	4
Compression Strength	[MPa]	3
Thermal Conductivity	[$Wm^{-1}K^{-1}$]	~ 7
Young module	[GPa]	2-3

Table 2.2 SiC foam properties (ErbiSiC foam, 10 PPI, source: Erbicol SA)

Erbicol produced foam samples with different cell orientation because it is well known that cell orientation affects both thermal conductivity and mechanical properties, which are important properties for application of foams in TPS. Enough material for tests and analysis was provided to the partners. Other samples with dimensions of 30x30x15 mm, 10 PPI, to study the adhesion between the CMC skins and foams and for re-entry tests simulations were produced. A better interface between foams and CMC was facilitated smoothing the edges of the foams.

Subsequently, Erbicol reduced the content of free silicon in foams, optimizing the microstructure but keeping mechanical and thermal properties above the threshold. Excess free silicon can cause material degradation at high temperature, given his relatively low melting point of 1414°C.

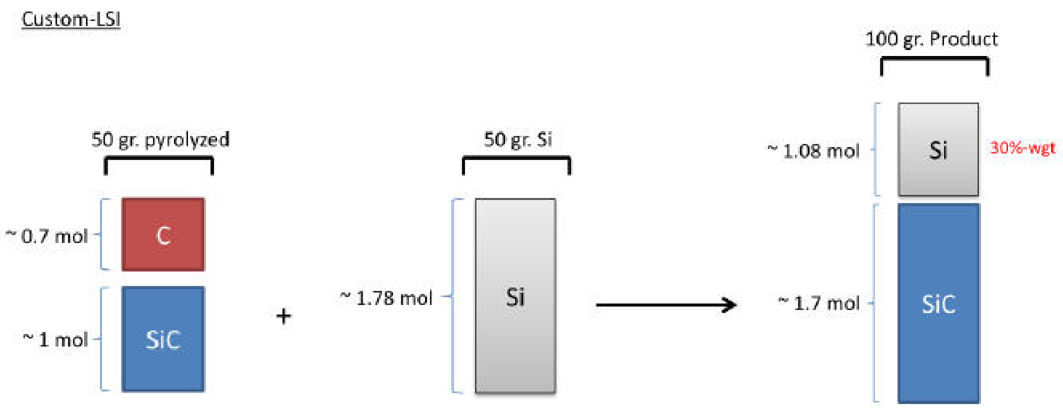

Figure 2.8. Calculation for standard Si-SiC foams

The optimization of the silicon content in the end product took into account the reaction bonding, the amount of silicon needed to form the matrix, thermal and mechanical properties. Following pictures show different sample after the LSI optimization.

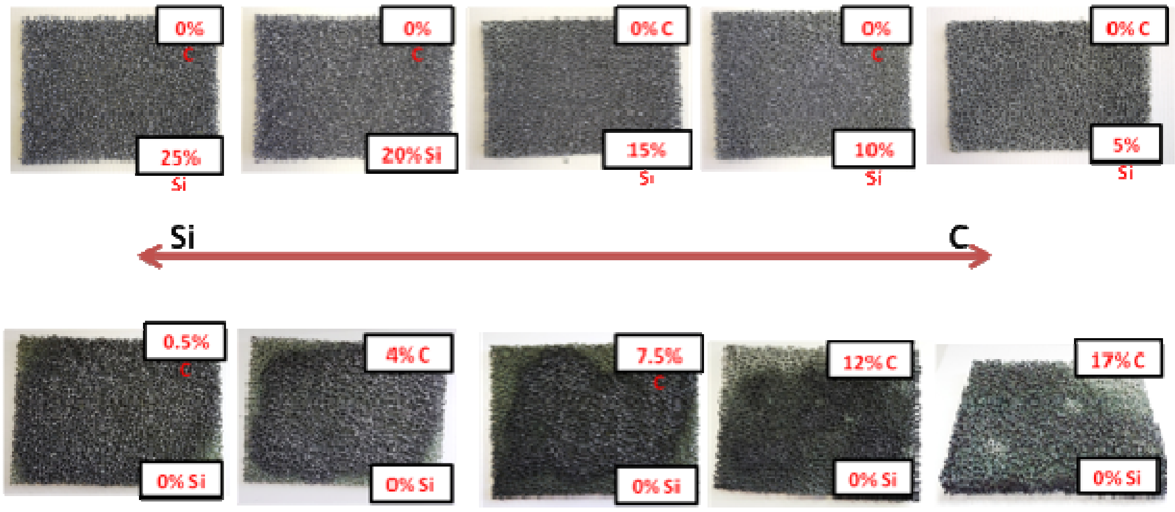

Figure 2.9. Foams with different content of silicon and carbon

After the products were validated at Supsi, EADS and POLITO, parameters were fixed and Erbicol manufactured the samples needed for the assembly with the CMC skins at EADS. These foams were produced using pure silicon (99.8% of purity) to further optimize the quality of the product.

a) b) c)

Figure 2.10. a) pure silicon; b) LSI preparation ; c) final result

It was found that a thermal stabilization treatment for the final product was beneficial for its stability during the subsequent assembly step. Therefore all products were stabilized by performing thermal shocks over a porous burner.

Figure 2.11. 50x50x10-15 mm samples during thermo shock;

To increase the insulation capacity of SiC cellular structure, a production method for hierarchical foams was developed. As a second insulating phase Fibremax™ bulk fibres (UNIFRAX Niagara Falls USA) were utilized. Fibres characteristics are reported in Table 2.3.

Fibre	
Fibre diameter [μm]	4-6
Composition:	
Al_2O_3	72%
SiO_2	27%
Fe_2O_3 Trace	0.02%
TiO_2 Trace	0.001%
MgO	0.05%
CaO	0.05%
Na_2O_3	0.10%
Specific heat [J kg^{-1} $°C^{-1}$]	1172
Felt	
Density	0.13
Thermal Conductivity [$Wm^{-1}K^{-1}$]	
@ 800	0.18
@ 1000	0.25
@ 1200	0.36

Table 2.3 Physical properties of the oxide fibre insulating phase (Fibremax®) from product datasheet.

Figure 2.12**Figure** shows the process employed to fill the foam. A dispersion of short fibres was forced to pass through the foams' pores. Fibres were stopped at the bottom of the foam by a filtering medium. To obtain the dispersion, 0.06 wt% of surfactant (Triton X100, Aldirch D) was diluted in distilled water, then short oxide fibres (5.7 wt.%) were added and dispersed by ball milling for 80 minutes.

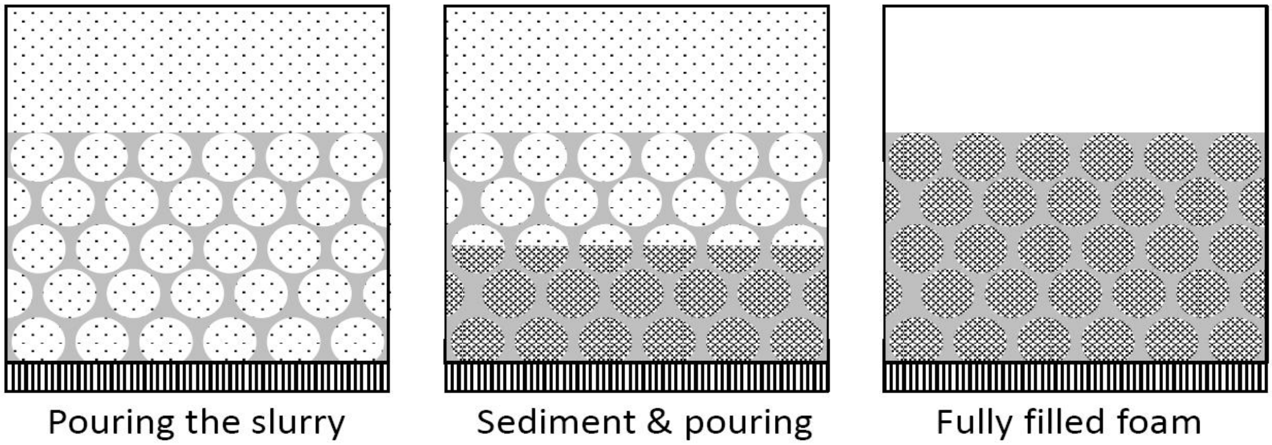

Figure 2.12 SiSiC foam filling via forced sedimentation: fibres dispersion pouring, water draining and fibres sedimentation and further pouring. The procedure was repeated till reaching the complete filling of the MRC body.

Foams were laid on a filter paper and a metallic net placed at the bottom of a metallic case surrounding the foam. The dispersion was then poured into the case and forced to pass by gravity through the SiSiC foam and the filter. The fibres, stopped by the filter, started to compact from the bottom of the foam. This forced sedimentation let the fibres layer grow inside the foam. The dispersion was poured several times until the entire foam was filled with short fibres.

Figure 2.13 On the left a 50x50 [mm] sandwich tile produced filling reticulated SiSiC with oxide fibres. On the right a close view of the foam showing the complete filling of the macroporosity.

The fibres amount into the dispersion and the filter pore size were optimized in order to fill the foams with the fibres (Figure .13). For the following thermal loading tests, six samples were produced, their properties are reported in Table 2.4.

sample #	foam					Oxide fibres		system
	Mass [g]	L [mm]	w [mm]	t [mm]	□ [g cm^{-3}]	□ 10^{-4} [g cm^{-3}]	w% [-]	□ [g cm^{-3}]
1	5.18	30.02	29.94	15.20	0.38	3.27	0.43	0.66
2	5.28	30.00	30.20	14.75	0.40	2.69	0.37	0.63
3	5.59	30.04	30.10	15.04	0.41	1.96	0.29	0.58
4	4.92	30.00	30.00	15.25	0.36	2.84	0.41	0.61
5	5.91	30.06	29.86	14.93	0.44	1.96	0.27	0.61
6	5.69	30.20	30.18	15.12	0.41	2.12	0.31	0.59

Average	5.43	30.05	30.05	15.05	0.40	2.47	0.35	0.61

Table 2.4 MRC, FRCI and HCC weights volumes and related properties before and after the forced sedimentation process.

3. CMCs suitable to act as skin of SiC foams in a sandwich structure and designed for providing toughness and strength

Within the SMARTEES novel technological applications were turned out with respect to joining of ceramic matrix composite (CMC) materials to ceramic foams. With C_f/SiC and SiC_f/SiC two different types of CMC materials have been evaluated. Furthermore different SiSiC ceramic foam types with respect to varying (tailored) Si content were used for the development of integrated $CMC_{upper\ skin}$ - SiSiC foam - $CMC_{lower\ skin}$ sandwich structures and its optimization in terms of achieving best mechanical performance and the criteria ‘non-failure of the brittle SiSiC foam’ over the complete assembly process and during loads. Finally a suitable process for the integration of $CMC_{upper\ skin}$ - SiSiC foam - $CMC_{lower\ skin}$ sandwich structures with excellent mechanical performance (bending strength, tensile strength, bonding at interface CMC/foam) was developed, see Figure 2.14.

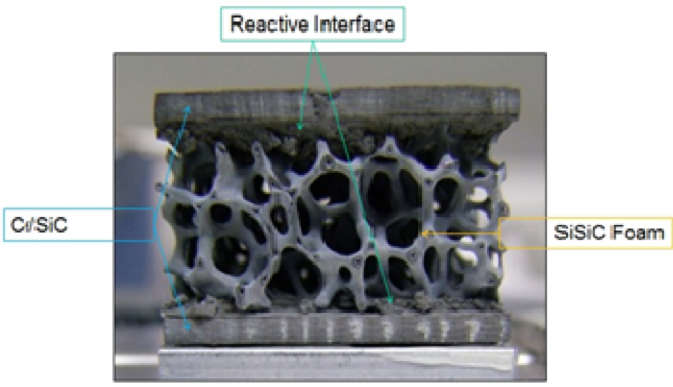

Fig. 2.14 Integrated C_f/SiC - SiC foam - C_f/SiC sandwich structure

The specific results refer to the following:

- Process development for joining dissimilar ceramic materials such as CMC materials with ceramic foam
- Ability to join dissimilar ceramic materials, in particular non-oxide CMC materials (C_f/SiC, SiC_f/SiC) with SiC & SiSiC based ceramic foams of varying Si content
- Development of a suitable slurry in order to join non-oxide CMC materials with ceramic foams SiSiC by chemical reaction (reaction bonding) between CMC (here mainly C_f/SiC), slurry constituents (e.g. binder, Si, C, SiC, additives) and ceramic SiSiC foam with varying Si content
- Application of the slurry material in the interface between the CMC and the ceramic foam in order to achieve a sound joint

- Ability to improve the mechanical performance of the joint by surface modification of the CMC and/or the ceramic foam
- Development of a suitable curing process using autoclave technique in order to guarantee good and homogeneous connection between CMC and ceramic foam
- Development of an high temperature treatment process based on Liquid Silicon Infiltration (LSI) technology in order to achieve chemical reaction between CMC (here mainly C_f/SiC), slurry constituents (e.g. binder, Si, C, SiC, additives) and ceramic SiSiC foam with varying Si content
- Improvement of LSI process and its parameters (atmosphere, gas flow, temperatures, temperature ramps, end temperature, time, sample placement including tooling etc.) in order to guarantee best mechanical performance of the CMC (here mainly C_f/SiC) / ceramic SiSiC foam (with varying Si content) joint
- Ability to fabricate CMC (here mainly C_f/SiC) / ceramic SiSiC foam joints and integrated CMC (here mainly C_f/SiC) / ceramic SiSiC foam / CMC (here mainly C_f/SiC) sandwich structures
- Ability to characterize the CMC (here mainly C_f/SiC) / ceramic SiSiC foam joints and integrated CMC (here mainly C_f/SiC) / ceramic SiSiC foam / CMC (here mainly C_f/SiC) sandwich structures, e.g. mechanical testing (bending, tensile)
- Ability to up-scale the developed process for the fabrication of CMC (here mainly C_f/SiC) / ceramic SiSiC foam joints and integrated CMC (here mainly C_f/SiC) / ceramic SiSiC foam / CMC (here mainly C_f/SiC) sandwich structures

WP3 Joining processes

The activities carried-out in WP3 refer to the definition, development and application of the bonding processes for the joining of the different parts of the Thermal Protection System (TPS) structure, i.e.

a) joining of a ceramic matrix composite material (CMC) that consists of carbon fibers embedded in a silicon carbon matrix a SiC matrix (C_f/SiC) to SiC based ceramic multilayers (SiC ML) for the external part of the TPS structure.
b) joining of the CMC to the metallic part for the internal part of the TPS.
c) the integration of SiC multilayer, CMC and metallic frame by joining for the whole TPS.

The output of this work was used for the construction of the technology samples in WP5.

The selection of the bonding processes, in order to comply with the TPS requirements investigated under WP1 and the environmental specifications and technology sample basic design, was carried out under WP3.1 and the outcome is described in deliverable D3.1 document.

The investigations that have been carried out so far give the following conclusions regarding the definition of the bonding processes

1) SiC ML multilayer to CMC joining

A number of routes have been selected and investigated for joining the CMC to SiC based ceramic multilayer for the external part of the TPS that can withstand temperatures as high as 1500 ºC.

From the investigated routes the diffusion bonding process employing $TiSi_{1.5}C_2$ as powder filler metal was selected as the most promising one. A series of joints were fabricated for various fabrication parameters, metallographically and structurally characterized and selected joints were mechanically and thermally tested for their performance. The optimization of the bonding process referred mainly a) to the proper pressure selection for the diffusion bonding process and b) to the elimination of cracks that appear on the surface of the SiC ML and extend from the filler area up to the free SiC surface, vertically to the joint interface. Reduction of cracks was achieved and their existence was proven not to be detrimental for the performance of the TPS under ground field relevant conditions. The optimised joining process gives sound joints which have, for the envisaged application, the appropriate thermomechanical properties at temperatures as high as 1794 °C. Fig. 3.1 depicts the cross section of the SiC ML-C_f/SiC fabricated using 25 MPa pressure.

However, the upscaling of the joining process to the size of 150×150 mm^2 for the technological sample resulted in warping of the joint at the periphery. For that reason an alternative route, based on graphite high temperature adhesive accompanied by appropriate surface modification of the surfaces to be joined, was investigated and used as an alternative solution. The cross section of the adhesive bonding of the SiC M to CMC s depicted in Fig.3.2.

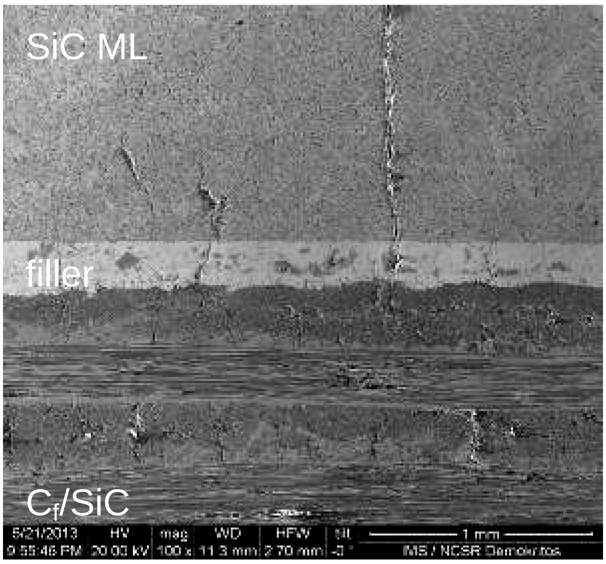

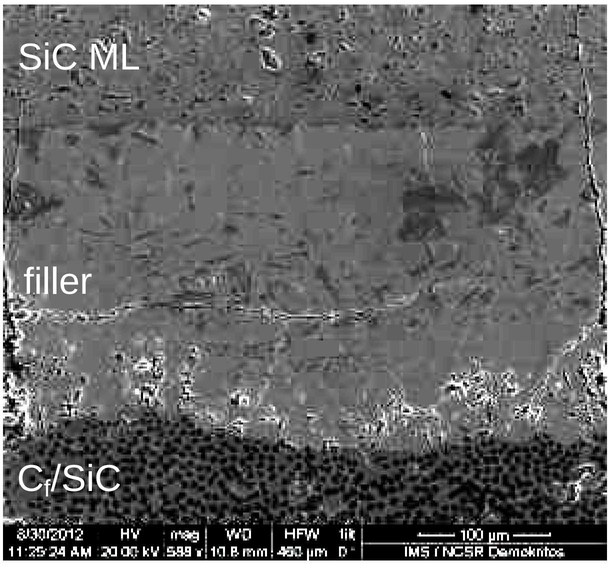

Fig.3.1. SEM micrographs of the cross section of the SiC ML-C_f/SiC joint fabricated at 25 MPa at magnification ×100 (left) and ×600 (right).

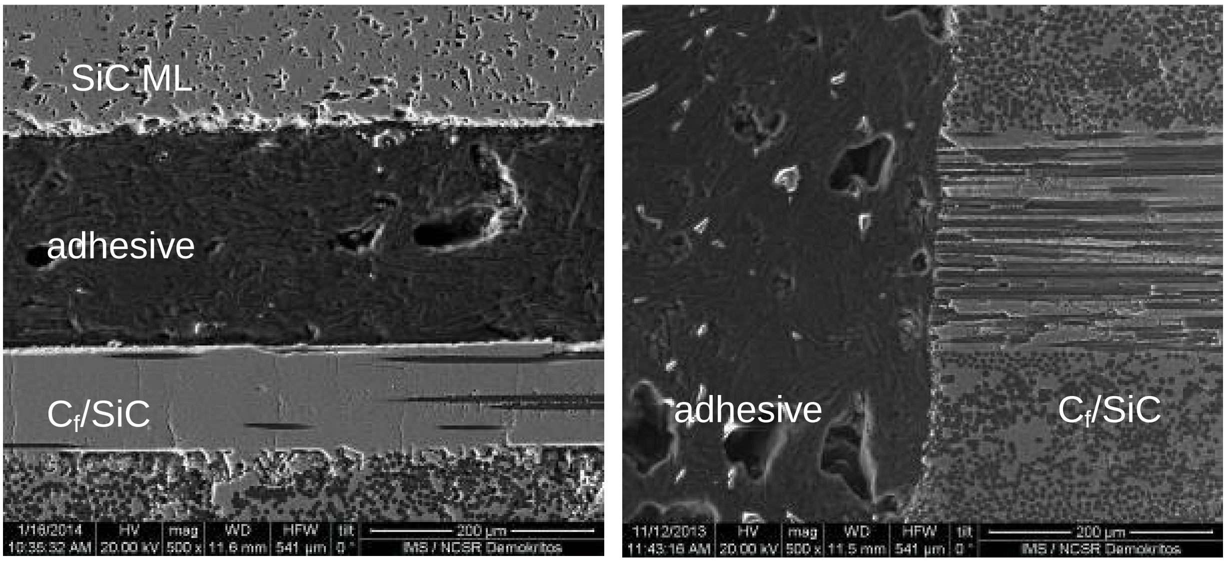

Fig.3.2. SEM micrographs of the cross section of the SiC ML-C_f/SiC joint using high temperature adhesive depicting all the interfaces (left) and the adhesive-C_f/SiC (right).

2) CMC to Ti alloy joint

The CMC to metal frame joining refers to the internal part of the TPS and the requirement is to withstand temperatures up to about 700 ºC maximum. The route that was selected within WP3.1 as the most promising one is based on brazing employing TiCuAg filler metal and perforation of the CMC. The joining process was optimized for the a) the brazing parameters (brazing temperature, holding time), b) the perforation geometry (hole diameter and depth) and c) filler type (foil, paste and powder). A series of joints were fabricated and metallographically investigated employing SEM with EDX analysis. Also the cross sections were structurally characterized by X-ray diffraction measurements. In general TiCuAg filler metal wets both parts and crack free brazed areas are produced. In most cases small cracks appear inside the CMC parallel to the interface, most often between the first and second interlayer. These cracks are always trapped between the vertical cracks, which are inherent in the CMC and which do not allow the propagation of the parallel to the interface cracks.

Two titanium alloys were investigated, Ti6Al4V-grade 5 and Ti-beta-21s. The latter, although it presents higher service temperature and enhanced oxidation resistance than Ti6Al4V, was rejected due to its beta transus at 800 ºC (transformation from hexagonal to cubic phase), about 100 ºC below the liquidus temperature of the TiCuAg filler metal. In addition the microstructural investigation of CMC/Ti-beta-21s joints have shown lengthy cracks in the first interlayer of the CMC.

Figs. 3.3 and 3.4 present the cross sections of the perforated CMC/Ti alloys joints.

Furthermore CMC/Ti alloys joints were fabricated for mechanical tests in the temperature range 25 to 600 ºC and for thermal cycling tests under re-netry conditions at a maximum temperature of 840 and 675 ºC. The maximum shear strength of 7.4 MPa achieved at 600 °C for the CMC to Ti alloy joint is adequate for the envisaged application and comparable to that of the CMC. In addition, the CMC/Ti joints survived 50 re-entry cycles with temperature at the CMC surface with no change in the microstructure of the joint (Figs. 3.5 and 3.6). Small cracks that are observed around the peripheral perforation of the CMC, in the post test analysis of the joints, are trapped in between the most peripheral holes and cannot propagate through the whole length of the joint.

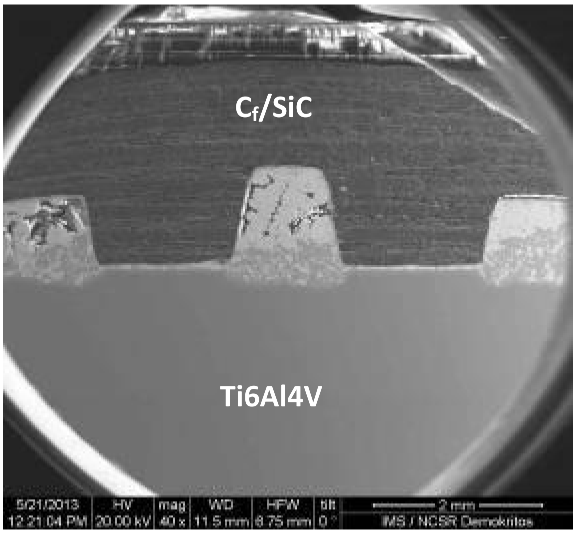

Fig.3.3. Cross of the perforated C_f/SiC-Ti6Al4V joint.

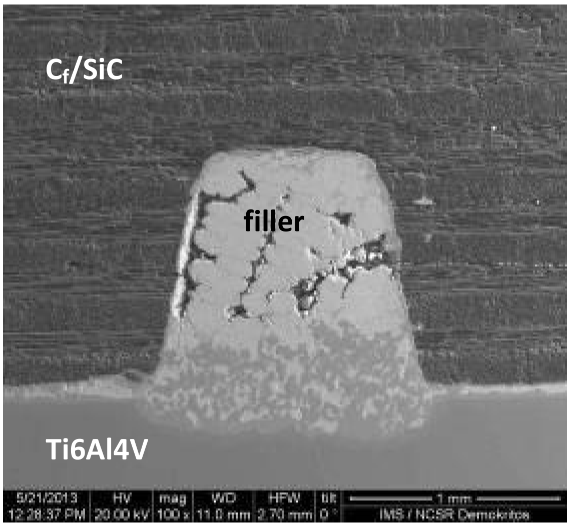

Fig.3.4. Micrograph of the cross of the perforated C_f/SiC-Ti6Al4V joint.

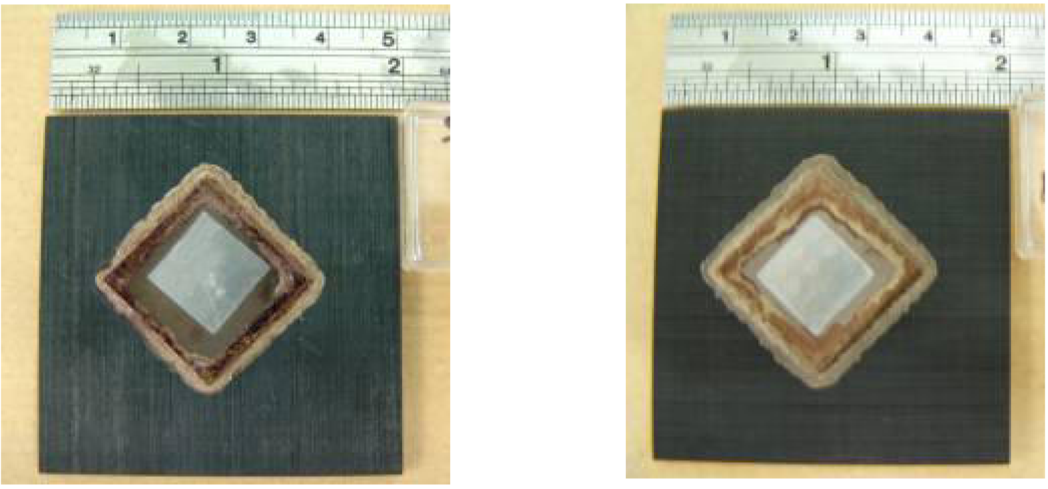

Fig.3.5. The CMC/Ti joints before the re-entry cycles.

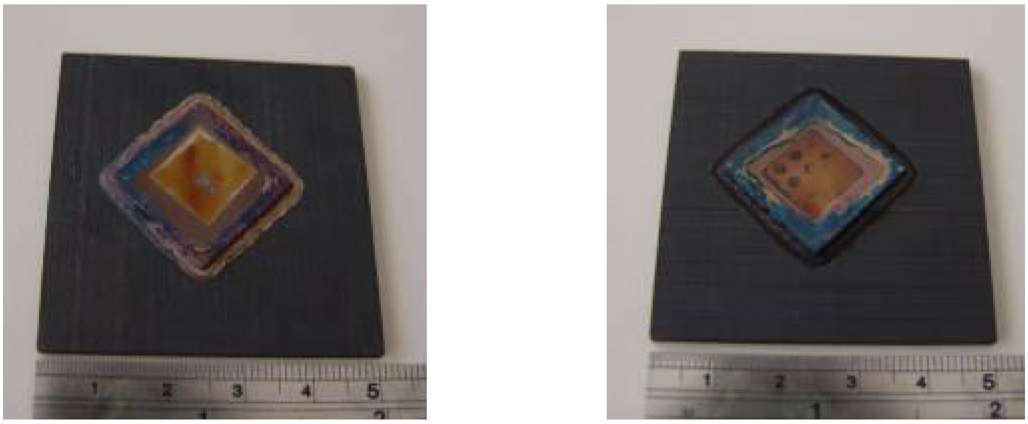

Fig.3.6. The CMC/Ti joints after 50 re-entry cycles at two heat loads.

The integration of the two types of joints in the TPS structure is depicted in Fig. 3.7, which shows a SiC multilayer joint to the CMC skin. The SiC/CMC joint was subsequently used to bond the foam between SiC/CMC upper structure with the lower CMC.

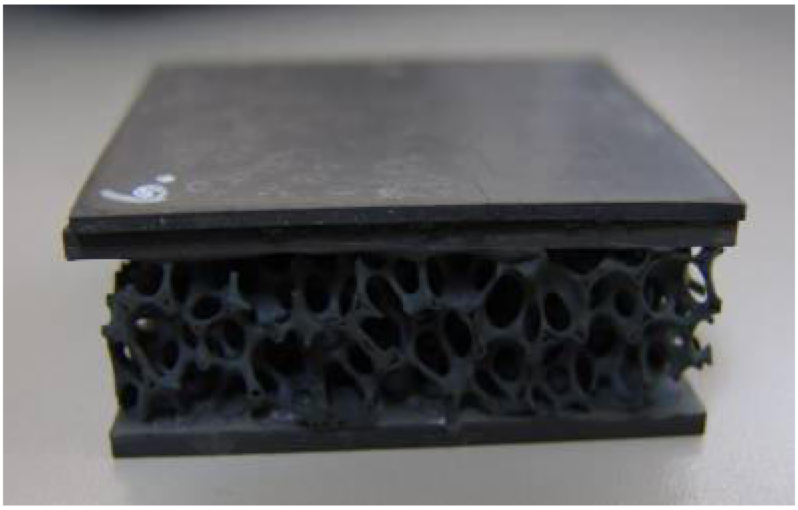

Fig.3.7. SiC/CMC/foam/CMC integration.

<u>WP4 Simulation</u>

In order to understand the mechanical behaviour of the sandwich for the TPS system, a X-Ray computed acquirement was performed on a sample. This was composed of an Erbicol Si-SiC foam and a SiC_f/Si-SiC CMC. Reconstruction and segmentation is performed with AVIZO software.

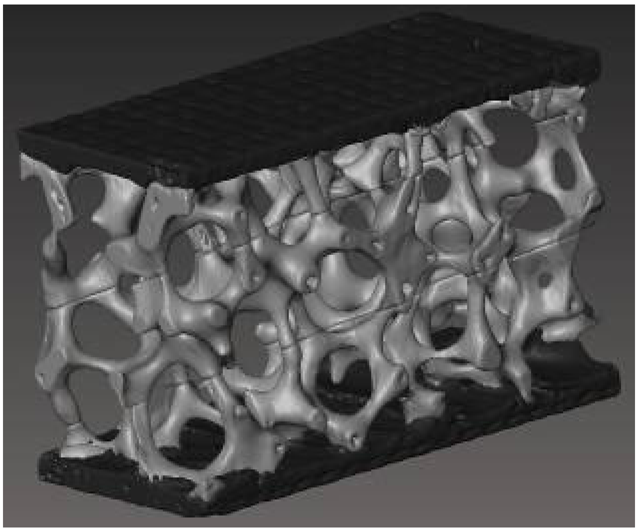

Figure 4.1. XCT + image processing (AVIZO) was fundamental to better understand the skin to core bonding and the mechanism that provides the load transfer from the skins to the core.

First mechanical analysis

When subjected to the thermal loading during re-entry structures are locally bending. For this reason the design phase was started with a mechanical analysis under bending varying parameters like skins thickness and intrinsic stiffness (Young module) one at a time. This was done in order to understand how normal and shear stresses arise inside the sandwich in a similar loading condition at ambient temperature (Figure 4.2).

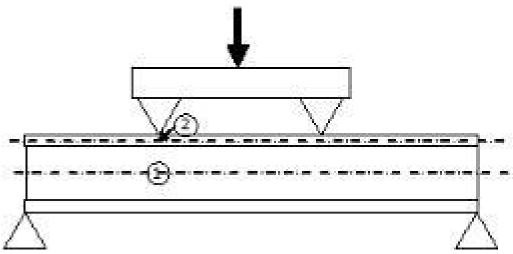

Figure 4.2. Bending set up Image shows the acquirement points for shear (1) and normal stresses

Figure 4.3. shows how shear stresses become dominant for stiffer ply configurations. Both elastic module and skin thickness (that act at forth power due to static moment of inertia) increase shear stresses into the system. This confirms the results obtained in experimental tests, were a prevalent shear failure mode is observed these structures..

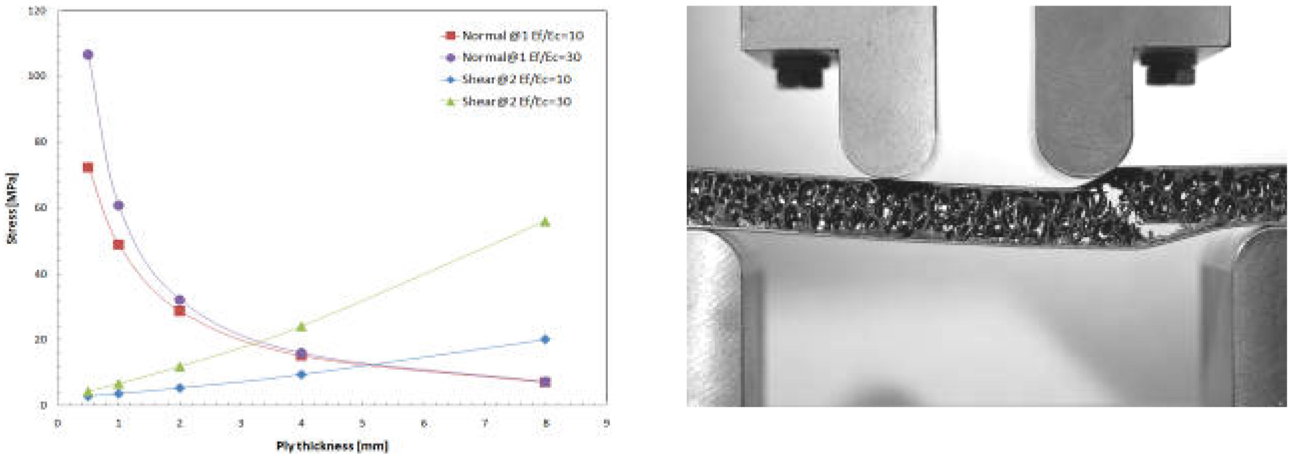

Figure 4.3. Left: stress values inside the sandwich VS skins thickness, right sandwich failure because of shear stresses.

This work allowed us to minimize the range of this two parameters' values for the following phase

TPS design

The final TPS design was obtained with iterative thermo mechanical finite element analysis (COMSOL Multiphysics).

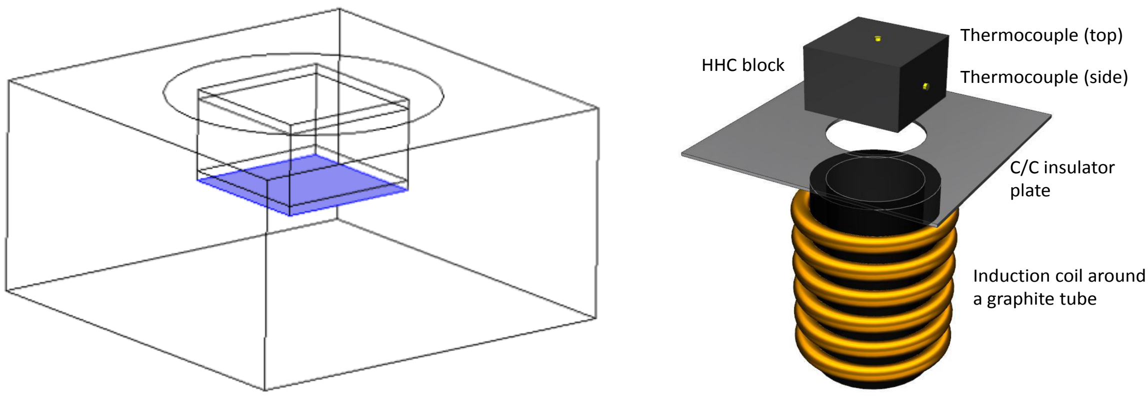

Simulation model

Experimental set-up

Figure 4.4. Simulation calibration: model and experimental set-up

A calibration of the thermal insulation properties of the filled sandwich was executed crossing results from AAC's thermal tests, since in a first simulation campaign, a relevant mismatch between analytically obtained properties and experimental data was observed.

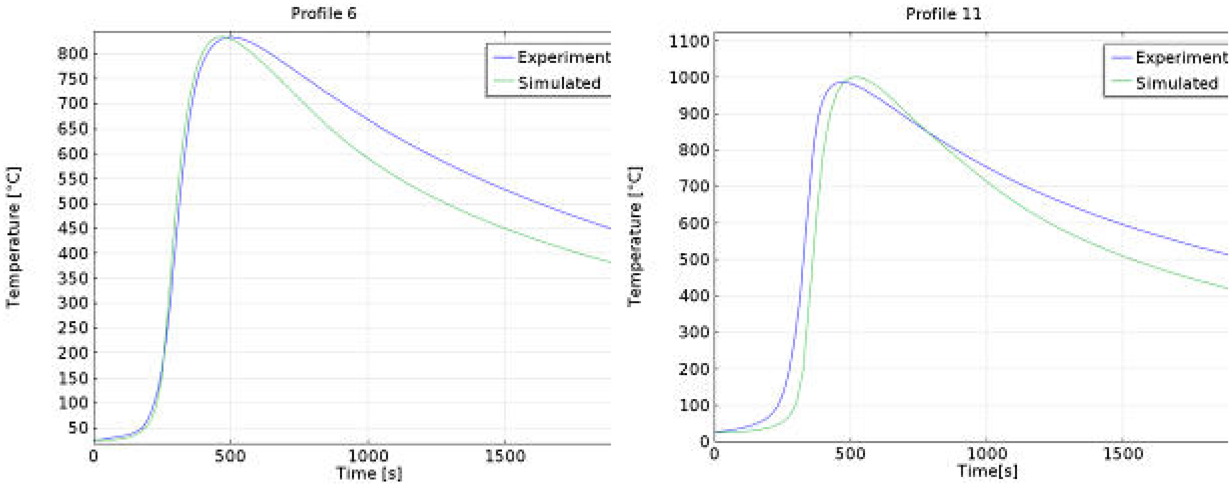

Figure 1.5. Model calibration with experimental results: a) Backside sample temperature profiles (load case 1) and b) Backside sample temperature profiles (Load case 2)

Thermal conductivity vs temperature behaviour was inferred by slight modifications of the specific heat capacity (given volumetric quantities of the foam and filler). A “more insulating” solution was obtained leading to an optimization of the previous design. In order to reproduce real testing condition of the system, the insulating walls used at AAC where added to the model in order to duplicate also lateral heat dissipation (Figure 4.5).

In the present report two TPS solutions for Load Case 1 and Load Case 2 are proposed.

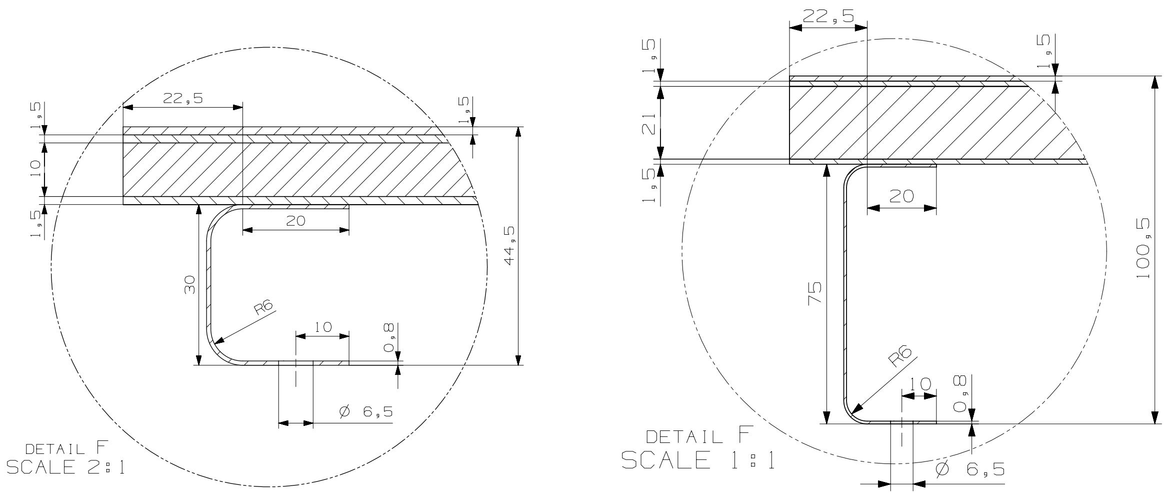

Load case 1 Load case 2

Figure 4.6. TPS final TPS configuration for the two load cases

Thermal insulation capability was the first design criteria for these final solutions. An important design constraint was also the areal mass that should be kept below mission requirements. For both load cases this requirement was not fulfilled taking into account the mass of each sub component. Insulation limitations were observed at the titanium-CMC interface where temperature has to be kept below the temperature of 816°C, and the surface of the vehicle structure temperature (150°C) (Figure 4.7).

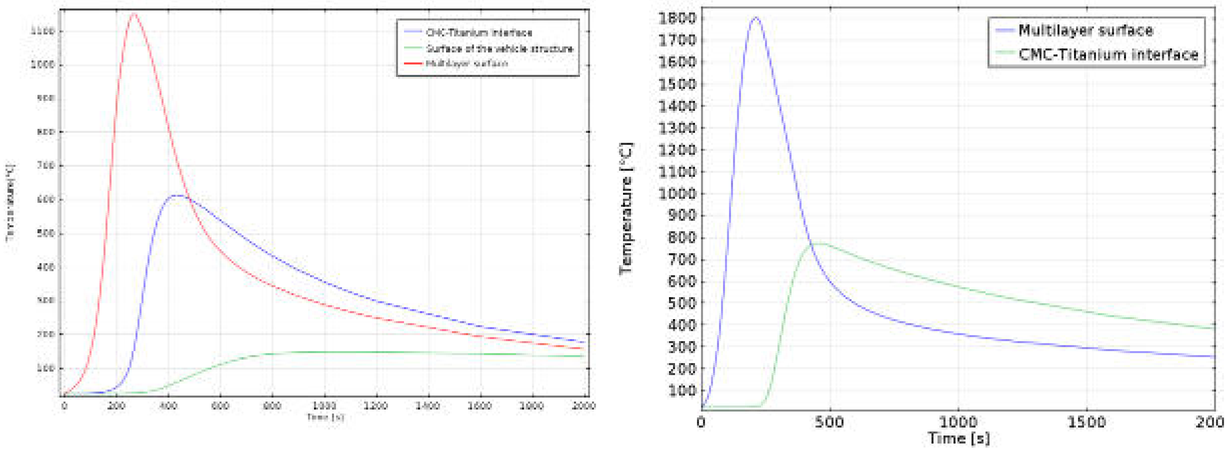

Load case 1 Load case 2

Figure 4.7. Temperature profiles of the complete structure under load case 1 (left) and 2 (right)

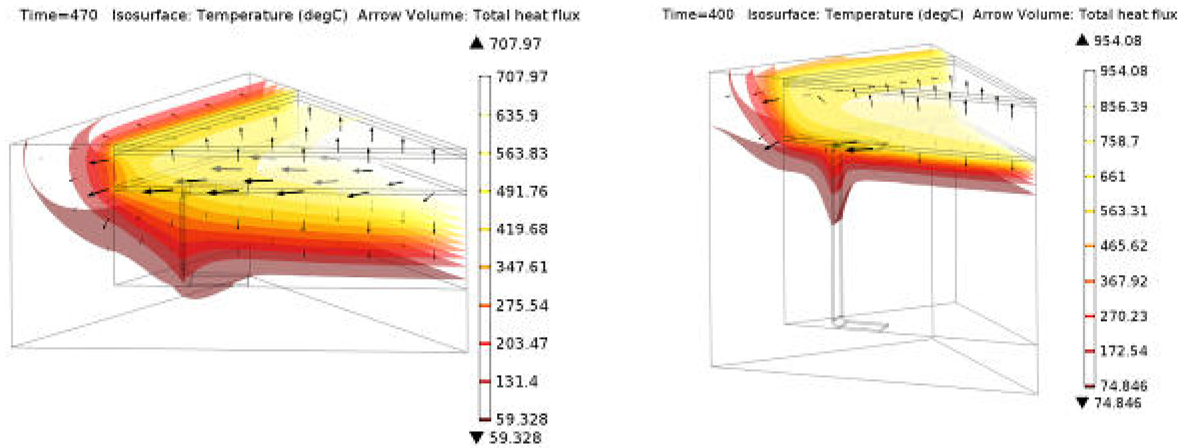

Load case 1 Load case 2

Figure 4.8. Thermal analysis contours: iso-temperature surfaces and heat flux path arrows (logarithmic scaled) for the two load cases at the end of the heat flux loading.

In Load Case 2 the very slow heat dissipation of the system to the exterior of the TPS during the “cold” phase of the re entry, allowed heat to propagate through the TPS to the vehicle (temperature of 149°C after 10000[s]). Taking this into account the height of the standoffs separating the sandwich from the primary structure was fixed at 75[mm]. This solution impacted negatively on the areal mass and reduced the first eigen frequencies of the structure which became less rigid. On the other hand the temperature of the surface should be kept below a critical value. Thermal-stress simulations showed that stresses exceed the intrinsic limit in almost each component (Figure 4.9) , due to the relevant thermal expansion mismatches.

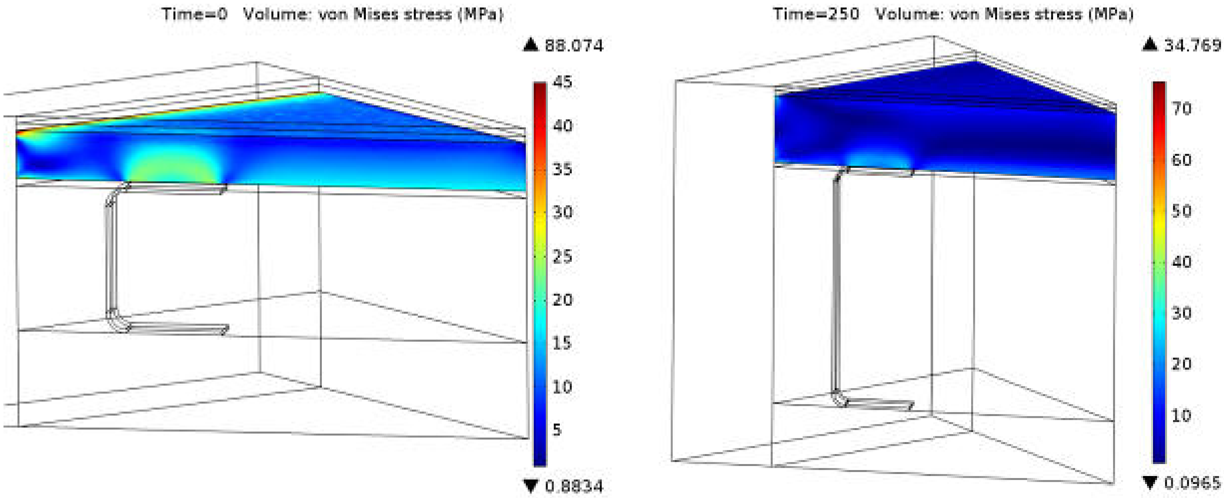

Load case 1 Load case 2

Figure 4.9. Von Mises stress contours in the ceramic foams for load case 1 (left) and 2 (right)

At the end of the project some materials properties, first taken from the literature, were made available after characterization (e.g. Emissivity). These were introduced into the model (as a function of the temperature) and simulations re-run.

Results in Figure 4.10 show that calculated temperature were previously over estimated giving further chances to obtain lighter and better performing solutions.

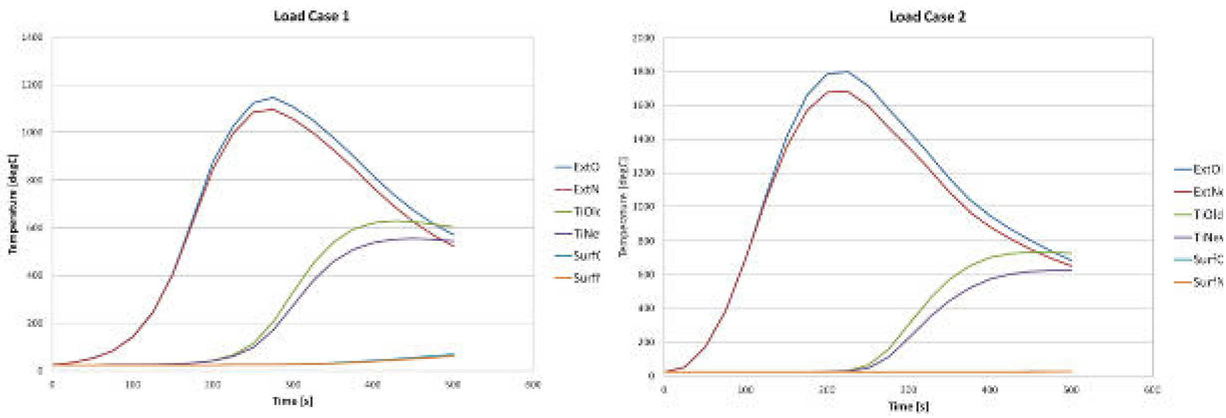

Figure 4.10 Temperatures distribution along the TPS before and after input properties modification.

WP5 TPS technology samples assembly

Ti alloy stand offs using the commercial Ti6Al4V grade 5 alloy were fabricated for the two selected thermal load cases.

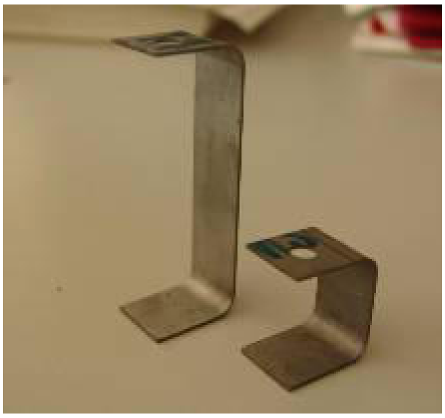

Fig. 5.1. The Ti stand off for load case 1 and 2.

In the upscaled technological samples having dimensions of 50×50 and 150×150 mm^2 the joining processes developed and optimised in WP3 were applied. Also filler metal $Ti_3Si_{1.5}C_2$ was fabricated for use in the upscaled SiC/CMC joints.

Specifically for the thermal load case 1 and 2 for samples having dimensions 50×50 mm^2 the joining processes for both SiC/CMC, CMC/foam/CMC and CMC/Ti alloy joints have been successfully applied as it is depicted in Figs. 5.2 and 5.3.

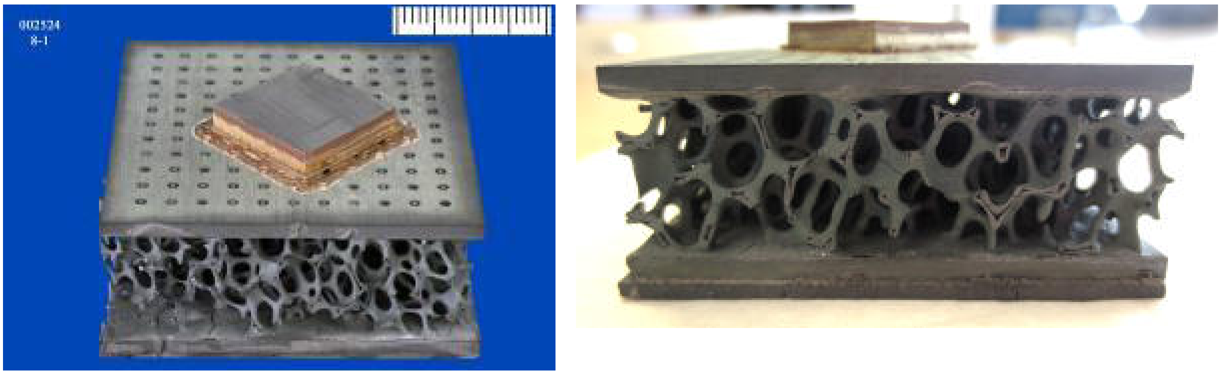

Fig.5.2. The technology sample 50 $\times$ 50 mm^2 for load case 1 showing the integration of all parts.

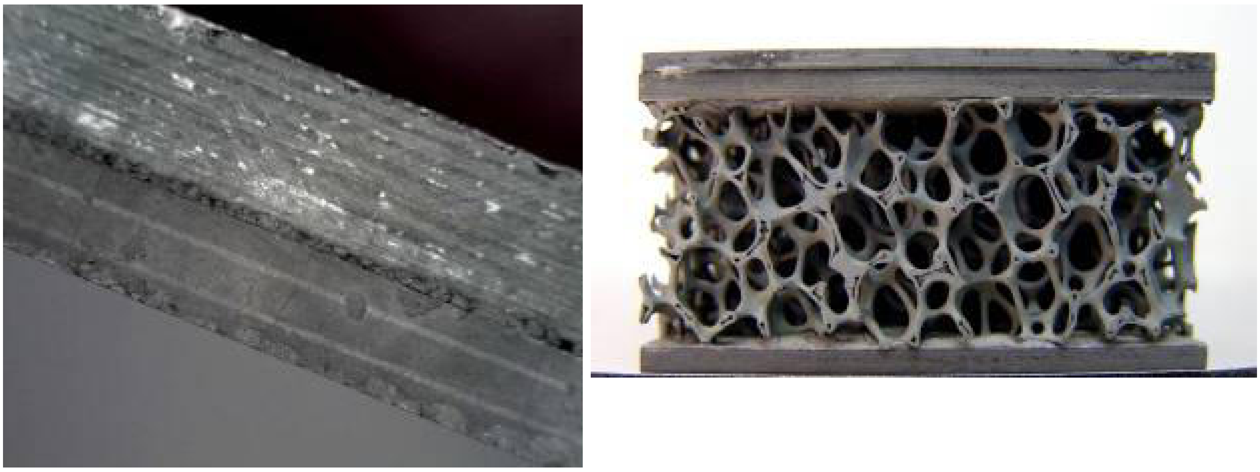

Fig.5.3. The technology sample 50×50 mm^2 for load case 2 showing the SiC/CMC interface (left) and the integration of SiC, CMC/foam/CMC sandwich (right).

During the upscaling of the technology sample to the size of 150×150 mm^2 difficulties were faced at the level of

a) Joining SiC multilayer to CMC. Warping of the joint prevented its use in the integration with the foam and the bottom part of the CMC

b) Joining of the Ti stand offs due to the loss of the temperature control in the furnace used (a furnace outside the consortium partners was employed, due to technical problems in the brazing furnace at TECNALIA, and it proved to be inappropriate for the brazing process).

The above two problems were resolved as follows

a) For the SiC/CMC joint the alternative route based on high temperature adhesives was applied

b) The brazing process of the Ti stand offs was applied successfully at TECNALIA’s furnace as can be seen in Fig. 5.4.

Fig.5.4. The technology sample 150 × 150 mm^2 for load case 2 after the brazing process of the Ti stand offs.

WP6 Ground testing and validation

The objective of this workpackage was the provision of ground testing facilities for representative load case for the selected flight application.

The overall work can be summarised as follows:

- In the 1st project year, improvements and adaptations of the test facility had to be performed, including test and calibration runs.
- Initial tests on SiC based foams delivered by ERBICOL performed under relevant thermal loads in order to assess the limits of these key components of the TPS
- In the 2nd project year, and based on these results, the open pore and filled foam samples from ERBICOL had been investigated, making clear that the pore filling enhances the suitability for TPS application substantially
- Joined Ti/CMC samples from DEMOKRITOS and TECNALIA were then investigated
- followed by tests on joined C/SiC / Multilayer Plates from DEMOKRITOS and TECNALIA

- Regarding the joined plates, no damage could be observed after applying heat fluxes equivalent to 1,391 °C and 1,794 °C. Further test were performed at a concentrated heat-flux (see description below).

- In the 3rd year, the improved joints of Ti/CMC delivered by DEMOKRITOS and TECNALIA were successfully characterised under all relevant load cases

- Joints of Multilayers (SiC based with and without ZrB2 interlayers) joined to CMC had been tested, indicating thermally induced stresses in the multilayer. The applied thermal gradients were however too high and beyond the real load case in a TPS

- CMC/Foam/CMC sandwiches delivered by EADS-IW had been fully characterised, indicating that these joints are not undergoing relevant degradation even when tested under loads exceeding the initially defined design limits

- Finally, a full assembly (small sample for load case 1) had been successfully tested, and the suitability of the selected concept, the selected materials, and the applied joining technology had been demonstrated

Summarising all the aforesaid, it shall be concluded that the development of all the materials and processes was successful:

For the foams, substantial decomposition of the ceramic filler and partial melting of the foam itself is observed at the 2 highest thermal loads (equivalent to 2,053 °C and 2,163 °C) only. This is not to be regarded as detrimental for the application, as such temperatures are not expected for the load cases the TPS has been designed.

The substantial improvements of Ti/CMC joints, manufactured with different brazes and different mechanical pre-treatment of the CMC plates, had been demonstrated. While initial specimens revealed substantial scattering, the final ones showed good strength and reliability, even at temperatures beyond the design load.

Regarding the multilayers, a relevant flux gradient (calculated by the end user), concentrated in the central part of the sample was applied in order to load the samples under a realistic thermal gradients. The multilayers passed the test, even at low oxygen environment.

The multilayer/CMC samples also passed the same type of test.

No problems were found on the CMC/Foam/CMC sandwiches assemblies.

Regarding the CMC/Ti joints, and extrapolation with data from WP4 was employed to use the relevant heat flux/ temperatures corresponding to this part/height of the TPS and the temperature of the test was increased till failure occurred (above 800 ºC).

Thus, at the end of the project, the SMARTEES team had been able to deliver all necessary materials, processes, and joining technologies for a TPS panel. Though only a load case 1 subscale panel had actually been tested, it may be assumed from the test results that the project objectives may directly be transferred to the originally foreseen panel dimensions.

The potential impact (including the socio-economic impact and the wider societal implications of the project so far) and the main dissemination activities and exploitation of results

The efforts towards enable a strong impact of the project where not only addressed to the scientific community (indexed paper and technical conferences and the EU citizen in general (webpage entries, short communication in newspapers, EU space conferences and brochures, but also to the space industry stake holders (technical workshops, news in Aerospace clusters and so on).

Concerning dissemination activities the following figures are highlighted:

- 10 sound paper at indexed journals
- 11 lectures at international technical conferences
- 11 dissemination activities to the public in general (news, poster, media, etc..)
- 2 Master/PhD thesis, arising from the results of the project and another 3 on going
- Scientific/technical workshop with relevant international experts and researchers.

Figure 2 shows figure and captions of few relevant dissemination activities the showcase in the 7th European Workshop on TPS & Hot Structures at ESA (2012, the poster at the 2nd FP7 space conference (2012) and the short news at the Spanish newspaper “La Razon” in 2013 and as an example of follow-up dissemination events a sample exposition at the kick off meeting for the new European Framework Programme for Research and Innovation “Horizon 2020”, in the frame of the incoming Greek Presidency of the European Council. SMARTEES was present at an exposition named “From Science to Technology”.

Un escudo espacial robusto de más de un uso

Belén Tobalina • Madrid

Tecnalia está trabajando en desarrollar una solución que permita proteger a los vehículos orbitales en su reentrada a la atmósfera. Se trata de un escudo térmico reutilizable que tendrá unas 30.000 «tejas» pequeñas y que permitirá proteger exteriormente al vehículo orbital frente al calor que se genera por el rozamiento con el aire. «Hasta ahora el único vehículo reutilizable que ha estado en servicio ha sido el Transbordador Espacial de Estados Unidos (STS). Sin embargo, su alto coste de mantenimiento, como las críticas recibidas tras el accidente del «Challeger», en 1986, y «Columbia», en 2003, hizo que desde entonces las misiones que requieren un retorno desde la estación internacional se realicen con la cápsula de la nave rusa «Soyuz», que permite un único uso», explican desde Tecnalia, empresa que junto con otros seis centros y compañías, están trabajando en el proyecto Smartees.

Esta solución plantea dos ahorros. El primero, al reducir los costes derivados del material y la reutilización. «Si comparamos los materiales empleados en el transbordador espacial reutlilizable con los de la cápsula Apollo, de un solo uso, a igualdad de superficie de protección térmica, éstos son un 60 por ciento más costosos que aquéllos. A esto hay que sumar también el ahorro que supone el poder utilizar el material más de una vez. El segundo ahorro tiene que ver con los costes de mantenimiento. El transbordador espacial estaba compuesto por unas 25.000 losetas de protección, pero se calculaba que un 30 por ciento de ellas se reparaban tras cada uso. Smartees ofrecerá una solución más robusta, que reducirá estos costes y que permitirá así su reutilización, cuando tras los citados accidentes, antes estos escudos quedaban inutilizados.

Figure 2: Selection of pictures and sketches of dissemination items: a) exposition at the 7th European Workshop on TPS & Hot Structures (ESTEC), b) Exposition for the H2020 launch event at the Greek Exhibition "From Science to Technology" at NCRSD, c) Poster at 2nd FP7 Space Conference (Cyprius, November 2012) and d) Press release at Spanish newspaper "La Razón" 24/02/13

Regarding the exploitation of the results

- Elaboration of an exploitation plan for each member of the consortium, also including non-space application.
- Specific use plan for the end user and industrial partners, including roadmaps, analysis of a value chain and technology transfer to other non-space products and applications (industry, energy, scientific infrastructure, etc…)

<u>**The address of the project public website**</u>

A a web site has been designed and constructed: www.smartees-project.eu, and keep updated in order to aid the dissemination activities (main publications and presentation are available for downloading). A use plan for each participant, with special emphasis on the industrial partners is released.

The website was divided in two different areas, one for public dissemination of the project and, the second one, only for project members (private area): Major dissemination items are available at the website for open downloading.

Contact points at eth website are:

- Dr. Jorge Barcena (Project Coordinator, jorge.barcena@tecnalia.com) and

- Mr. Jesus Marcos (Space and Defence market director, jesus.marcos@tecnalia.com)

In addition new tools such Google analytics, allows to monitor the visit to the webpage. Along the three years the website has received around 3,000 visits with an average duration of 3 minutes.